

Lyso-PAF Analogues and Lysophosphatidylcholines from the Marine Sponge *Spirastrella abata* as Inhibitors of Cholesterol Biosynthesis

Boo Ahn Shin,[†] Yu Ree Kim,[†] Ik-Soo Lee,[‡] Chung Ki Sung,[‡] Jongki Hong,[§] Chung J. Sim,[⊥] Kwang Sik Im,^{||} and Jee H. Jung*^{||}

College of Pharmacy, Pusan National University, Pusan 609-735, The Research Institute of Medical Sciences, Chonnam National University, Kwangju, College of Pharmacy, Chonnam National University, Kwangju, Korea Basic Science Institute, Taejon, and Department of Biology, Hannam University, Taejon, Korea

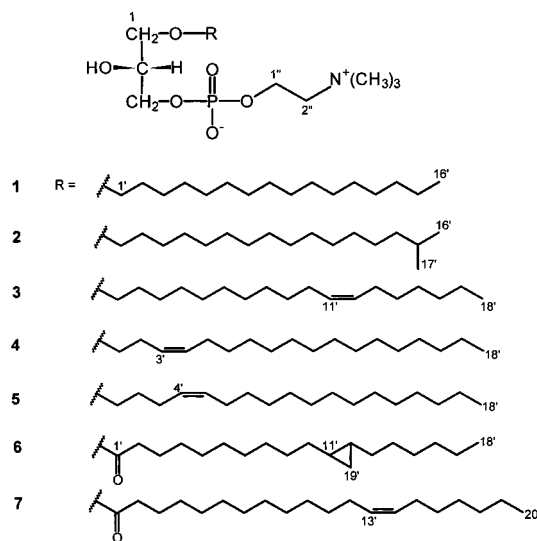
Received June 18, 1999

A series of phospholipids, including previously undescribed compounds **4**–**7**, were isolated by a bioactivity-guided fractionation from the marine sponge *Spirastrella abata* as inhibitors of cholesterol biosynthesis in human liver cells. These compounds were identified as lyso-PAF analogues (**1**–**5**) and lysophosphatidylcholines (**6**, **7**) based on NMR and MS analyses. Compounds **1**–**7** specifically blocked the conversion of lanosterol into cholesterol in the Chang liver cell.

Marine sponges of the genus *Spirastrella* are reported to contain various sterols,¹ picrotoxin,² a sphingosine derivative,³ 14,15-seco-curvularin,⁴ *ent*-3 β ,16 α -atisanediol,⁵ and spongistatins.⁶ In the course of searching for hypolipemic constituents from marine sponges, we have noticed significant activity in the crude extract of *Spirastrella abata* (Spirastrellidae) collected from Korean waters. A series of lysophosphatidylcholines and lyso-PAF (platelet-activating factor) analogues were isolated as inhibitors of cholesterol biosynthesis by a bioactivity-guided fractionation. The HMG-CoA reductase inhibitors such as lovastatin, simvastatin, and pravastatin are among the most widely used hypolipemics. The target enzyme, HMG-CoA reductase, is a rate-limiting enzyme in cholesterol biosynthesis. However, because it is not pathway-specific, the inhibition of this enzyme blocks the generation of other metabolites that are essential for the proper functioning of the human body, hence causing various side effects such as myositis,⁷ rhabdomyolysis, and renal dysfunction.⁸ In this regard, much interest has been shown in the development of more specific inhibitors, which exert inhibition at the late stages of the biosynthetic pathway. We have established an assay system modified from that of Gerst et al.⁹ to screen inhibitors of cholesterol biosynthesis. Unlike HMG-CoA reductase inhibitors, lysophosphatidylcholines and lyso-PAF analogues from *S. abata* suppressed the late stage of the cholesterol biosynthetic pathway, thus exerting more specific inhibition.

Employing a bioactivity-guided fractionation, the methanol extract of *S. abata* was subjected to successive solvent partitionings and chromatographies to afford a series of analogues (**1**–**7**) of which compounds **4**–**7** are previously undescribed. Compound **4** was isolated as an amorphous solid. FABMS of **4** showed a $[M + H]^+$ peak at m/z 508. The ¹H NMR spectrum showed methylene and methine proton signals integrated to 11 protons at δ 4.29–3.46 (Table 1) and a singlet signal integrated to nine protons at δ 3.22 (three *N*-methyl groups). In all, seven carbon signals attached to heteroatoms, including a triplet *N*-

methyl carbon signal, were observed at δ_C 72.9–54.7 (Table 2) in the proton-decoupled ¹³C NMR spectrum. Also the presence of a linear alkyl chain was indicated in the ¹H and ¹³C NMR spectra. By careful analysis of COSY and HMQC spectral data, a phosphatidylcholine skeleton was unraveled. Characteristic couplings (³*J*_{HP}) between protons (H-3) and phosphorus were observed (Table 1). Couplings between phosphorus and relevant carbons (C-2, C-3, C-1', and C-2'') (²*J*_{CP}, ³*J*_{CP}) were also observed (Table 2). The carbon (C-2'') vicinal to the quaternary ammonium nitrogen was further split into a triplet due to ¹³C–¹⁴N coupling. The two pairs of allylic protons of the alkyl chain were observed as two distinct signals (δ 2.32 and 2.06), and the olefinic protons showed a complex second-order splitting. Thus, it may be postulated that the double bond is located near the beginning or the end of the alkyl chain. Consecutive COSY correlations from H-1' to H-3' clearly showed that the double bond is located at C-3'. The geometry of the double bond was deduced to be *cis*, based on the chemical shifts of the allylic carbons (δ 28.8 and 28.3). The structure of **4** was therefore determined to be 1-*O*-(3'*Z*-octadecenyl)-*sn*-glycero-3-phosphocholine, while the stereochemistry at C-2 was deduced to be identical to that of **1**, which had been determined by comparing specific optical rotation with the reported data.^{10a}



* To whom correspondence should be addressed. Tel.: (8251) 510-2803. Fax: (8251) 510-2803. E-mail: jhjung@hyowon.cc.pusan.ac.kr.

[†] The Research Institute of Medical Sciences, Chonnam National University.

[‡] College of Pharmacy, Chonnam National University.

[§] Korea Basic Science Institute.

[⊥] Hannam University.

^{||} Pusan National University.

Table 1. ^1H NMR Spectral Data of **1** and **4–6** (δ , mult, J)^a

position	1	4	5	6
1	3.50 (dd, 10.0, 5.0)	3.52 (dd, 9.9, 4.9)	3.50 (dd, 10.0, 4.9)	4.16 (dd, 11.3, 4.4)
	3.45 (dd, 10.0, 5.6)	3.47 (dd, 9.9, 5.7)	3.45 (dd, 10.0, 5.7)	4.11 (dd, 11.3, 6.3)
2	3.89 (quint, 5.3)	3.89 (quint, 5.3)	3.89 (quint, 5.2)	3.97 (quint, 4.7)
3	3.94 (ddd, 10.0, 5.9, 3.6 ^b)	3.94 (ddd, 10.0, 6.0, 3.7 ^b)	3.94 (ddd, 10.0, 5.9, 3.7 ^b)	3.90 (m)
	3.85 (ddd, 10.0, 6.1, 6.1 ^b)	3.86 (ddd, 10.0, 6.0, 6.0 ^b)	3.85 (ddd, 10.0, 6.1, 6.1 ^b)	
1'	3.46 (t, 7.0)	3.46 (t, 6.7)	3.47 (t, 5.8)	
2'	1.57 (quint, 7.0)	2.32 (q, 6.9)	1.61 (quint, 7.2)	2.36 (t, 7.8)
3'	1.25–1.35 (m)	5.40 (m)	2.10 (q, 6.8)	1.62 (quint, 7.2)
4'	1.25–1.35 (m)	5.44 (m)	5.35 (m)	1.25–1.35 (m)
5'	1.25–1.35 (m)	2.06 (q, 6.9)	5.38 (m)	1.25–1.35 (m)
6'	1.25–1.35 (m)	1.25–1.35 (m)	2.04 (q, 7.0)	1.25–1.35 (m)
7'–9'	1.25–1.35 (m)	1.25–1.35 (m)	1.25–1.35 (m)	1.25–1.35 (m)
10', 13'	1.25–1.35 (m)	1.25–1.35 (m)	1.25–1.35 (m)	1.40 (m), 1.18 (m)
11', 12'	1.25–1.35 (m)	1.25–1.35 (m)	1.25–1.35 (m)	0.68 (m)
14', 15'	1.25–1.35 (m)	1.25–1.35 (m)	1.25–1.35 (m)	1.25–1.35 (m)
16'	0.90 (t, 6.8)	1.25–1.35 (m)	1.25–1.35 (m)	1.25–1.35 (m)
17'		1.25–1.35 (m)	1.25–1.35 (m)	1.25–1.35 (m)
18'		0.89 (t, 7.0)	0.90 (t, 6.8)	0.91 (t, 7.2)
19'				0.59 (td, 7.8 ^c , 3.6 ^d) –0.32 (td, 5.4 ^e , 3.6 ^d)
1''	4.29 (m)	4.29 (m)	4.29 (m)	4.29 (m)
2''	3.65 (m)	3.64 (m)	3.63 (m)	3.64 (m)
N-CH ₃	3.23 (s)	3.22 (s)	3.22 (s)	3.23 (s)

^a Spectra were recorded in CD₃OD at 600 MHz. ^b Denote ³J_{HP} values. ^c Cis coupling. ^d Geminal coupling. ^e Trans coupling.

Table 2. Proton-Decoupled ^{13}C NMR Spectral Data of **1**, **4**, and **6** (δ , mult, J)^a

position	1	4	6
1	72.9 (s)	72.9 (s)	66.3 (s)
2	71.0 (d, 7.6)	71.0 (d, 7.6)	69.9 (d, 7.6)
3	68.5 (d, 5.8)	68.5 (d, 6.1)	67.8 (d, 5.8)
1'	72.7 (s)	72.3 (s)	175.4 (s)
2'	30.8–30.4 (s)	28.8 (s)	34.9 (s)
3'	27.2 (s)	126.6 (s)	26.0 (s)
4'	30.8–30.4 (s)	132.8 (s)	31.3–29.9 (s)
5'	30.8–30.4 (s)	28.3 (s)	31.3–29.9 (s)
6'	30.8–30.4 (s)	30.8–30.4 (s)	31.3–29.9 (s)
7'–9'	30.8–30.4 (s)	30.8–30.4 (s)	31.3–29.9 (s)
10'	30.8–30.4 (s)	30.8–30.4 (s)	29.9 (s)
11', 12'	30.8–30.4 (s)	30.8–30.4 (s)	16.9 (s)
13'	30.8–30.4 (s)	30.8–30.4 (s)	29.9 (s)
14'	33.1 (s)	30.8–30.4 (s)	31.3–29.9 (s)
15'	23.7 (s)	30.8–30.4 (s)	31.3–29.9 (s)
16'	14.4 (s)	33.0 (s)	33.1 (s)
17'		23.7 (s)	23.7 (s)
18'		14.4 (s)	14.4 (s)
19'			11.6 (s)
1''	60.4 (d, 5.1)	60.4 (d, 4.9)	60.4 (d, 5.0)
2''	67.5 (dt, 7.2, 3.0 ^b)	67.5 (dt, 7.2, 3.0 ^b)	67.5 (dt, 7.2, 3.0 ^b)
N-CH ₃	54.7 (t, 3.9 ^b)	54.7 (t, 3.8 ^b)	54.7 (t, 3.8 ^b)

^a Spectra were recorded in CD₃OD at 50 MHz. Multiplicities represent ^{13}C – ^{31}P couplings otherwise indicated. ^b ^{13}C – ^{14}N coupling. ^c May be interchanged.

Table 3. Inhibition of **1–7** on the Cholesterol Biosynthesis in the Chang Liver Cells

compound	1	2	3	4	5	6	7
IC ₅₀ ($\mu\text{g}/\text{mL}$)	422	320	125	174	121	60	21

Compound **5** also contained one double bond in the alkyl chain but showed a slightly different ^1H NMR spectral pattern from that of **4**. Consecutive COSY correlations from H-1' to H-4' clearly showed that the double bond is located at C-4'. The location of the double bond was further confirmed by the FAB–CID–MS/MS of the $[\text{M} + \text{H}]^+$ ion (m/z 508) by observing prominent allylic cleavages at m/z 338 and 284 (major fragmentations were observed as odd-numbered fragment ions due to the remote charge fragmentation characteristic of the collisional activation). This fragmentation pattern was the same as that of **4** except for a 14-amu shift. Thus, the structure of **5** was determined to be 1-*O*-(4'*Z*-octadecenyl)-*sn*-glycero-3-phosphocholine.

Compound **6** showed NMR data rather different from those of **5**. A carbonyl carbon signal (δ_{C} 175.4) and an α -methylene proton signal (δ 2.36) were observed indicating the presence of an ester linkage instead of an ether linkage. The shift in the oxymethylene proton signals observed at δ 3.52 and δ 3.47 (H-1) in **4** to δ 4.16 and δ 4.11 further supported the fact. Also the characteristic proton and carbon signals arising from a cyclopropane moiety were observed (δ 0.68, 0.59, –0.32; δ_{C} 16.9, 11.6). The large difference between the chemical shifts of the ring geminal methylene protons and the large coupling constant between the ring methylene (H-19') and methine protons (H-11', 12') (triplet, 7.8 Hz) were clear indications that the cyclopropane ring was *cis*-disubstituted.¹¹ The FABMS of **6** showed a $[\text{M} + \text{H}]^+$ ion at m/z 536. The position of the cyclopropane moiety in the 1-*O*-acyl chain was deduced from the enhanced β -cleavages at m/z 464 and 396 in the FAB–CID–MS/MS of the $[\text{M} + \text{H}]^+$ ion, while other peaks in between appeared in much lower intensities. The relatively low intensity of the peak at m/z 478 (γ -cleavage) was also indicative of the position of the cyclopropane moiety.¹¹ Using a combination of COSY, HMQC, and FAB–CID–MS/MS data analyses, the structure of **6** was determined to be 1-*O*-(*cis*-11',12'-methyleneoctadecanoyl)-*sn*-glycero-3-phosphocholine.

Compound **7** showed NMR data similar to those of **6**. The presence of a double bond instead of a cyclopropane moiety in the alkyl chain was noticed. The location of the double bond was determined by FAB–CID–MS/MS analysis of the $[\text{M} + \text{H}]^+$ ion at m/z 550. Allylic cleavages were observed as enhanced peaks at m/z 478 and 424, indicating the location of the double bond at C-13'. The fragments at m/z 438 and 450 showed a 12 amu difference as relatively weak peaks, augmenting the evidence for the location of the double bond. Thus the structure of **7** was determined to be 1-*O*-(13'*Z*-eicosaenoyl)-*sn*-glycero-3-phosphocholine. Compounds **1–3** have been identified as known metabolites that have been previously reported from hydroids, earthworms, sea cucumbers, or sponges.¹⁰ The couplings of ^{31}P and ^{14}N to the relevant ^1H and ^{13}C of **1** were fully analyzed in this paper (Tables 1 and 2).

Compounds **4**, **5**, and **7** are chemically uncommon for their atypical location of the double bond in the alkyl chain,

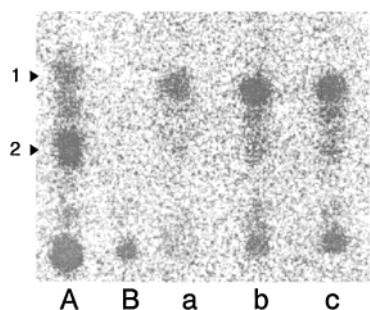


Figure 1. The effect of compound **6** on the cholesterol biosynthesis in the Chang liver cells analyzed by phosphor image analyzer. **1**: lanosterol, **2**: cholesterol; **A**: control; **B**: mevastatin; **a**, **b**, **c**: concentrations of **6** at 40 $\mu\text{g/mL}$, 20 $\mu\text{g/mL}$, and 10 $\mu\text{g/mL}$, respectively.

while **6** is unusual for its cyclopropane moiety in the acyl chain. Compounds **1**–**7** displayed inhibition of cholesterol biosynthesis in the Chang liver cell in a concentration dependent mode. Among these, lysophosphatidylcholines **6** and **7** exhibited higher potencies (Table 3). In the mevastatin (HMG-CoA reductase inhibitor) treated cells, the biosynthesis of all the major intermediate metabolites, including lanosterol and cholesterol, was notably suppressed (Figure 1, lane B). In contrast, **6** substantially suppressed the biosynthesis of cholesterol, while that of lanosterol was relatively unaffected, implying that **6** has specifically blocked the conversion of lanosterol into cholesterol.

Experimental Section

General Experimental Procedures. Melting points were determined on an Electrothermal melting point apparatus and are uncorrected. Optical rotation was measured on a JASCO DIP-1000 polarimeter. ^1H and ^{13}C NMR spectra were recorded on a Bruker AC200 or DMX600 spectrometer. Chemical shifts were reported in reference to the respective residual solvent peaks (δ 3.3 and δ_{C} 49.0 for CD_3OD). FABMS and FAB–CID–MS/MS data were obtained using a JEOL JMS–HX110/110A (four-sector instrument with a E1B1E2B2 configuration).

Animal Material. The sponge *Spirastrella abata* was collected by hand using scuba at a 13-m depth in November 1996, off Cheju Island, Korea.¹² The sponge grows as a thick plate attached to rocks. The surface of the sponge has slightly raised papillae and oscula that measures 0.5–1 mm in diameter at the end of the papillae. Live specimens are pale purple on the surface, but yellowish brown underneath.

Biological Evaluation. The Chang liver cells (ATCC CCL 13) derived from stock cultures were seeded at 5×10^4 cells in 15-mm diam plastic Petri dishes in 0.5 mL of medium containing MEM with 10% FBS. On the second day of culture, the cells were washed twice with serum-free media Hepatozyme–SFM (GibcoBRL) and cultured for 4 h. The cells were pretreated for 2 h with a given amount of the test compound. Labeled acetate (2.5 $\mu\text{Ci/well}$) was added to the culture medium. After 2 h of incubation, the medium was removed, and the dishes were washed three times with phosphate-buffered saline (pH 7.4). The cells were treated with 200 μL of 0.1 N NaOH and saponified with 6% KOH in MeOH (w/v), and the nonsaponifiable lipid was extracted with *n*-hexane. The *n*-hexane extract was developed on TLC (Merck Si gel 60F₂₅₄) with a solvent system of C_6H_6 – Me_2CO (19:1), and the radioactive spots were analyzed by a phosphor image analyzer (BAS-1500).

Extraction and Isolation. The frozen sponge (5.25 kg) was extracted with MeOH at room temperature. The MeOH-soluble fraction was partitioned between H_2O and CH_2Cl_2 . The CH_2Cl_2 -soluble fraction was further partitioned between 90% aqueous MeOH and *n*-hexane to yield 19.8 and 10.9 g of residues, respectively. The 90% aqueous MeOH fraction was subjected to a reversed-phase flash column chromatography (YMC Gel ODS-A, 60 \AA , 500/400 mesh) eluting with 33–100%

MeOH– H_2O followed by EtOAc to yield seven fractions (F1–F7). Fraction F4 (3320 mg), which eluted at 90% MeOH– H_2O was further separated by a reversed-phase flash column chromatography eluting with 88–100% MeOH– H_2O and Me_2CO into seven fractions (F4-1–F4-7). Fraction F4-5 (471 mg), which eluted at 88% MeOH– H_2O , was further purified on a reversed-phase HPLC (YMC ODS–H80, 250 \times 10 mm, S-4 μm , 80 \AA) eluting with 57% MeOH– H_2O to afford compounds **1** (18 mg) and **6** (1.7 mg). Both fractions F4-4 (350 mg) and F4-6 (821 mg) were combined (FM) and subjected to a MPLC (YMC Gel ODS-A, 120 \AA , 230 mesh) eluting with 75–95% MeOH– H_2O to afford 8 fractions (FM 1–8). Fraction FM 4 was further purified on a reversed-phase HPLC (YMC ODS–H80, 250 \times 10 mm, S-4 μm , 80 \AA) eluting with 88% MeOH– H_2O to afford **2** (5 mg), **3** (5 mg), and additional **1** (41 mg) and **6** (4 mg). Compounds **4**, **5**, and **7** were purified from fraction FM 5 by a reversed-phase HPLC (YMC–Pack CN, 250 \times 10 mm, S-5 μm , 120 \AA) eluting with MeOH– H_2O (1.3:1) yielding 4.4, 3.5, and 1.2 mg, respectively.

1-O-Hexadecyl-sn-glycero-3-phosphocholine (1): amorphous solid; mp 152 $^\circ\text{C}$ (dec); $[\alpha]_{\text{D}}^{25} -3.4^\circ$ (*c* 0.41, MeOH); ^1H NMR, see Table 1; ^{13}C NMR, see Table 2; FABMS m/z 482 $[\text{M} + \text{H}]^+$; FAB–CID–MS/MS m/z 482 (100), 466 (0.4), 452 (0.3), 438 (0.4), 424 (0.35), 410 (0.3).

1-O-(15'-Methylhexadecyl)-sn-glycero-3-phosphocholine (2): amorphous solid; ^1H NMR (CD_3OD , 200 MHz) δ 4.28 (2H, m, H-1'), 3.86 (3H, m, H-2, H-3), 3.63 (2H, m, H-2''), 3.45 (4H, m, H-1, H-1'), 3.21 (9H, s, *N*- CH_3), 1.56 (2H, quint, $J = 6.8$ Hz, H-2'), 1.48 (1H, m, H-15'), 1.35–1.25 (– CH_2 –), 0.87 (6H, t, $J = 6.4$ Hz, H-16', H-17'); ^{13}C NMR (CD_3OD , 50 MHz) δ_{C} 72.9 (C-1), 72.7 (C-1'), 71.0 (d, $J_{\text{CP}} = 7.6$ Hz, C-2), 68.5 (d, $J_{\text{CP}} = 5.8$ Hz, C-3), 67.5 (dt, $J_{\text{CP}} = 7.2$ Hz, $J_{\text{CN}} = 3.0$ Hz, C-2''), 60.4 (d, $J_{\text{CP}} = 5.1$ Hz, C-1'), 54.7 (t, $J_{\text{CN}} = 3.9$ Hz, *N*- CH_3), 40.2 (C-14'), 31.1–30.3 (– CH_2 –), 29.1 (C-15'), 28.5 (C-13'), 27.2 (C-3'), 23.0 (C-16', C-17'); FABMS m/z 496 $[\text{M} + \text{H}]^+$; FAB–CID–MS/MS m/z 496 (100), 480 (1.2), 466 (0.2), 452 (0.7), 438 (1.0), 424 (0.6).

1-O-(11'-Z-Octadecenyl)-sn-glycero-3-phosphocholine (3): amorphous solid; ^1H NMR (CD_3OD , 200 MHz) δ 5.33 (2H, t, $J = 4.9$ Hz, H-11', H-12'), 4.28 (2H, m, H-1''), 3.86 (3H, m, H-2, H-3), 3.63 (2H, m, H-2''), 3.45 (4H, m, H-1, H-1'), 3.21 (9H, s, *N*- CH_3), 2.02 (4H, q, $J = 5.9$ Hz, H-10', H-13'), 1.56 (2H, quint, $J = 5.0$ Hz, H-2'), 1.35–1.25 (– CH_2 –), 0.89 (3H, t, $J = 7.0$ Hz, H-18'); ^{13}C NMR (CD_3OD , 50 MHz) δ_{C} 130.85, 130.84 (C-11', C-12'), 72.9 (C-1), 72.7 (C-1'), 71.0 (d, $J_{\text{CP}} = 7.6$ Hz, C-2), 68.5 (d, $J_{\text{CP}} = 6.1$ Hz, C-3), 67.5 (dt, $J_{\text{CP}} = 7.2$ Hz, $J_{\text{CN}} = 3.0$ Hz, C-2''), 60.4 (d, $J_{\text{CP}} = 4.9$ Hz, C-1'), 54.7 (t, $J_{\text{CN}} = 3.8$ Hz, *N*- CH_3), 33.0 (C-16'), 30.9–30.0 (– CH_2 –), 28.10, 28.13 (C-10', C-13'), 27.2 (C-3'), 23.7 (C-17'), 14.4 (C-18'); FABMS m/z 508 $[\text{M} + \text{H}]^+$; FAB–CID–MS/MS m/z 508 (100), 492 (0.55), 478 (0.3), 464 (0.35), 450 (0.35), 436 (0.4), 422 (0.3), 408 (0.2), 396 (0.2), 382 (0.7), 368 (0.4).

1-O-(3'-Z-Octadecenyl)-sn-glycero-3-phosphocholine (4): amorphous solid; ^1H NMR, see Table 1; ^{13}C NMR, see Table 2; FABMS m/z 508 $[\text{M} + \text{H}]^+$; FAB–CID–MS/MS m/z 508 (100), 492 (1.3), 478 (1.0), 464 (1.4), 450 (1.5), 436 (1.4), 324 (0.5), 270 (0.2).

1-O-(4'-Z-Octadecenyl)-sn-glycero-3-phosphocholine (5): amorphous solid; ^1H NMR, see Table 1; FABMS m/z 508 $[\text{M} + \text{H}]^+$; FAB–CID–MS/MS m/z 508 (100), 492 (1.0), 478 (0.8), 464 (1.2), 450 (1.3), 436 (1.4), 338 (0.8), 284 (1.2).

1-O-(cis-11',12'-Methylene-octadecanoyl)-sn-glycero-3-phosphocholine (6): amorphous solid; ^1H NMR, see Table 1; ^{13}C NMR, see Table 2; FABMS m/z 536 $[\text{M} + \text{H}]^+$; FAB–CID–MS/MS m/z 536 (100), 520 (0.3), 506 (0.2), 492 (0.2), 478 (0.1), 464 (0.2), 450 (0.1), 436 (0.1), 424 (0.1), 410 (0.1), 396 (0.3).

1-O-(13'-Z-Eicosaenoyl)-sn-glycero-3-phosphocholine (7): amorphous solid; ^1H NMR (CD_3OD , 200 MHz) δ 5.33 (2H, t, $J = 4.9$ Hz, H-13', H-14'), 4.29 (2H, m, H-1''), 4.13 (2H, m, H-1), 3.96 (1H, quint, $J = 4.9$ Hz, H-2), 3.90 (2H, m, H-3), 3.64 (2H, m, H-2''), 3.22 (9H, s, *N*- CH_3), 2.35 (2H, t, $J = 8.0$ Hz, H-2'), 2.03 (4H, q, $J = 5.9$ Hz, H-12', H-15'), 1.61 (2H, q, $J = 7.0$ Hz, H-3'), 1.35–1.25 (– CH_2 –), 0.91 (3H, t, $J = 7.0$ Hz, H-20'); FABMS m/z 550 $[\text{M} + \text{H}]^+$; FAB–CID–MS/MS m/z 550

(100), 534 (0.8), 520 (0.3), 506 (0.4), 492 (0.4), 478 (0.4), 424 (1.5), 410 (0.5).

Acknowledgment. The authors thank Ji Yun Kim, Boua Kim, Hyun Soo Kim, and Jung Kun Kim for their sincere assistance in collection and laboratory work. High resolution (600 MHz) NMR spectra were provided by the Korea Basic Science Institute. This study was supported by the grants from Pusan National University and the Ministry of Health and Welfare (HMP-96-D-1-1008).

References and Notes

- (1) (a) Das, B.; Srinivas, K. V. N. S. *J. Nat. Prod.* **1992**, *55*, 1310–1312. (b) Das, B.; Rao, S. P.; Srinivas, K. V. N. S. *J. Nat. Prod.* **1993**, *56*, 2210–2211. (c) Kailidini, R. S. H. S. N.; Rao, C. B. S.; Akihisa, T.; Tamura, T.; Matsumoto, T. *Ind. J. Chem.* **1988**, *27B*, 160–162.
- (2) Sarma, N. S.; Rambabu, M.; Anjaneyulu, A. S. R.; Rao, C. B. S. *Ind. J. Chem.* **1987**, *26B*, 189–190.
- (3) Garg, H. S.; Agrawal, S. *J. Nat. Prod.* **1995**, *58*, 442–445.
- (4) Abrell, L. M.; Borgeson, B.; Crews, P. *Tetrahedron Lett.* **1996**, *37*, 8983–8984.
- (5) Cafieri, F.; Fattorusso, E.; Mahajnah, Y.; Mangoni, A. *Magn. Reson. Chem.* **1995**, *33*, 286–289.
- (6) (a) Pettit, G. R.; Herald, C. L.; Cichacz, Z. A.; Gao, F.; Schmidt, J. M.; Boyd, M. R.; Christie, N. D.; Boettner, F. E. *J. Chem. Soc., Chem. Commun.* **1993**, 1805–1807. (b) Pettit, G. R.; Cichacz, Z. A.; Herald, C. L.; Gao, F.; Boyd, M. R.; Schmidt, J. M.; Hamel, E.; Bai, R. *J. Chem. Soc., Chem. Commun.* **1994**, 1605–1606.
- (7) (a) Norman, D. J.; Illingworth, D. R.; Munsen, J.; Hosenpud, J. *New Engl. J. Med.* **1988**, *318*, 46–47. (b) Smith, P. F.; Eydeloth, R. S.; Grossman, S. J.; Schwartz, M. S.; Germershausen J. I.; Vyas, K. P.; Kari, P. H.; MacDonald, J. S. *J. Pharmacol. Exp. Ther.* **1991**, *257*, 1225–1235.
- (8) (a) Corpier, C. L.; Jones, P. H.; Suki, W. N.; Lederer, E. D.; Quinones, M. A.; Schmidt, S. W.; Young, J. B. *JAMA*, **1988**, *260*, 239–241. (b) Spach, D. H.; Bauwens, J. E.; Clark, C. D.; Burke, W. G. *West. J. Med.* **1991**, *154*, 213–215.
- (9) Gerst, N.; Duriatti, A.; Schuber, F.; Taton, M.; Benveniste, P.; Rahier, A. *Biochem. Pharmacol.* **1988**, *37*, 1955–1964.
- (10) (a) Fusetani, N.; Yasukawa, K.; Matsunaga, S.; Hashimoto, K. *Comp. Biochem. Physiol.* **1986**, *83B*, 511–513. (b) Noda, N.; Tsunefuka, S.; Tanaka, R.; Miyahara, K. *Chem. Pharm. Bull.* **1992**, *40*, 2756–2758. (c) Butler, A. J.; Van Altena, I. A.; Dunne, S. J. *J. Chem. Ecol.* **1996**, *22*, 2041–2061. (d) Yayli, N.; Findlay, J. A. *J. Nat. Prod.* **1994**, *57*, 84–89. (e) Iorizzi, M.; Minale, L.; Riccio, R.; Higa, T.; Tanaka, J. *J. Nat. Prod.* **1991**, *54*, 1254–1264.
- (11) Murakami-Murofushi, K.; Shioda, M.; Kaji, K.; Yoshida, S.; Murofushi, H. *J. Biol. Chem.* **1992**, *267*, 21512–21517.
- (12) The sponge was identified by Prof. Chung Ja Sim, Department of Biology, Hannam University. A voucher specimen (J96J-3) was deposited in the Natural History Museum, Hannam University, Taejeon, Korea.

NP990303A